Enhancing UAV Propulsion: Insights into Toroidal Propeller Dynamics through CFD Simulations

Oliveira L. Nícolas[1], Hallak H. Patrícia[2], Lemonge C. de C. Afonso[3]

[1]*Postgraduate program in computational modeling - Federal University of Juiz de Fora*
Campus Universitário, Rua José Lourenço Kelmer, s/n - São Pedro, Juiz de Fora - MG, Brazil, 36036-900
nicolas.lima@ufjf.br
[2]*Department of applied and computational mechanics - Federal University of Juiz de Fora*
Campus Universitário, Rua José Lourenço Kelmer, s/n - São Pedro, Juiz de Fora - MG, Brazil, 36036-900
patricia.hallak@engenharia.ufjf.br
[3]*Department of applied and computational mechanics - Federal University of Juiz de Fora*
Campus Universitário, Rua José Lourenço Kelmer, s/n - São Pedro, Juiz de Fora - MG, Brazil, 36036-900
afonso.lemonge@ufjf.br

Abstract. Unmanned Aerial Vehicles (UAVs) are increasingly used in various fields, but noise pollution remains a significant issue. A novel toroidal propeller design by MIT Lincoln Laboratory aims to address this by reducing vortex-induced drag and enhancing stiffness, thus lowering noise without sacrificing thrust or adding extra weight. This paper proposes an aerodynamic optimization of a toroidal propeller through CFD simulations, obtaining a optimized propeller 7% more efficient than the original geometry.

Keywords: Propellers, toroidal, aerodynamics, optimization, CFD

1 Introduction

A novel propeller design developed by MIT Lincoln Laboratory addresses the noise issues associated with small multirotor unpiloted aircraft, or drones. The toroidal propeller features a unique structure where two blades loop together, reducing the drag effects of vortices and enhancing the overall stiffness of the propeller. This design significantly lowers the acoustic signature of drones, making them less of a noise disturbance. The propeller not only maintains thrust levels comparable to conventional designs but also achieves this without requiring additional components that would increase weight and power consumption. This innovation has the potential to accelerate the acceptance of drones in various applications, including aerial deliveries, cinematography, industrial inspections, and agricultural monitoring, by making them quieter and more efficient [1]. In Figure 1, it is possible to compare the acoustic pressure of the proposed propeller with a conventional propeller.

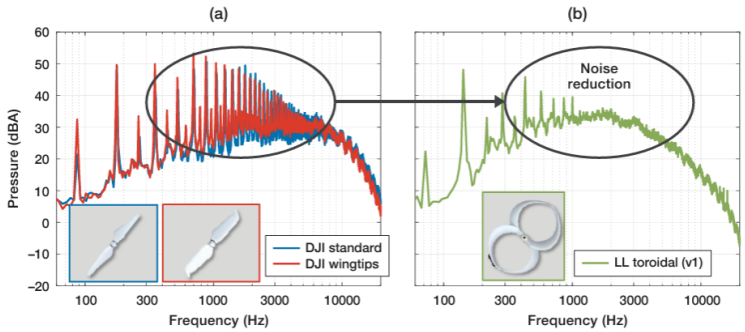

Figure 1. Acoustic pressure comparison between standard propeller and MIT proposed propeller

As it is an novel proposal for an aeronautical propeller, little research has been conducted on the subject, and there are not many publications available. Vu *et al.* [2] proposes an in-depth numerical analysis of aerodynamic

and aeroacoustic properties of toroidal propeller designs aimed at reducing noise and enhancing performance. The study examines four different propeller geometries, focusing on the reduction of blade tip vortices and the stabilization of airflow. Results demonstrate that the Tri-loop Toroidal propeller achieves optimal efficiency in terms of thrust and acoustic power level. This research highlights the potential for noise reduction and performance improvements in drone applications through advanced propeller design. Gabriel & Simion [3] explore the design, fabrication, and performance of a quadcopter with 3D-printed toroidal propellers. The toroidal shape is expected to enhance aerodynamic efficiency over conventional designs. Finite element analysis (FEA) simulated the propeller's behavior under various loads, while ANSYS Fluent software evaluated thrust performance. The study offers insights into the benefits of toroidal propellers and 3D printing for efficient quadcopter development.

2 Propeller performance parameters

The performance parameters of a propeller are usually dimensionless. According to Brandt and Selig [4], the efficiency of a propeller is given by:

$$\eta = J\frac{C_T}{C_P} \tag{1}$$

where J is a nondimensionalisation of the velocity called the advance ratio and given by:

$$J = \frac{V}{nD} \tag{2}$$

where V, n, and D are, respectively, the forward speed, rotation, and diameter of the propeller.

The coefficients of thrust (C_T) and power (C_P) are defined as:

$$C_T = \frac{T}{\rho n^2 D^4} \tag{3}$$

$$C_P = \frac{P}{\rho n^3 D^5} \tag{4}$$

where ρ is the air density, T is the thrust generated, and P is the power the propeller absorbs.

A propeller's efficiency is given by:

$$\eta = \frac{C_T J}{C_P} \tag{5}$$

3 CFX/ANSYS - COMPUTATIONAL FLUID DYNAMICS

CFX is a computational fluid dynamics software from ANSYS. It is capable of solving the Navier-Stokes equations, given by:

- The continuity equation

$$\frac{\partial \rho}{\partial t} = \nabla.(\rho \mathbf{U}) \tag{6}$$

- The momentum equations

$$\frac{\partial(\rho \mathbf{U})}{\partial t} + \nabla.(\rho \mathbf{U} \times \mathbf{U}) = -\nabla p + \nabla.\tau \tag{7}$$

where t is time, and $\mathbf{U}$ is the velocity field, p is pressure, and τ is the stress tenso.

The turbulence model used was the $k-\omega$ model. It solves two transport equations, one for the turbulent kinetic energy k and one for the turbulent frequency ω:

- k - equation

$$\frac{\partial(\rho k)}{\partial t} + \frac{\partial}{\partial x_{\mathrm{j}}}(\rho \mathbf{U_j} k) = \frac{\partial}{\partial x_{\mathrm{j}}}[(\mu + \frac{\mu_{\mathrm{t}}}{\sigma_{\mathrm{k}}})\frac{\partial k}{\partial x_{\mathrm{j}}}] + P_{\mathrm{k}} - \beta^{'}\rho k\omega + P_{\mathrm{kb}} \tag{8}$$

- ω-equation

$$\frac{\partial(\rho \omega)}{\partial t} + \frac{\partial}{\partial x_{\mathrm{j}}}(\rho \mathbf{U_j} \omega) = \frac{\partial}{\partial x_{\mathrm{j}}}[(\mu + \frac{\mu_{\mathrm{t}}}{\sigma})\frac{\partial \omega}{\partial x_{\mathrm{j}}}] + \alpha\frac{\omega}{k}P_k - \beta\rho\omega^2 + P_{\mathrm{wb}} \tag{9}$$

The density, ρ, velocity vector, $\mathbf{U}$, are obtained using the Navier-Stokes method. P_{kb} and P_{wb} are production rates. α, β, β', and σ_k are model constants. The Reynolds tension tensor is calculated from the:

$$-\rho\overline{u_{\mathrm{i}}u_{\mathrm{j}}} = \mu_{\mathrm{t}}(\frac{\partial \mathbf{U}_{\mathrm{i}}}{\partial x_{\mathrm{j}}} + \frac{\partial \mathbf{U}_{\mathrm{j}}}{\partial x_{\mathrm{i}}}) - \frac{2}{3}\delta_{\mathrm{ij}}(\rho k + \mu_{\mathrm{t}}\frac{\partial\, \mathbf{U}_{\mathrm{k}}}{\partial x_{\mathrm{k}}}) \tag{10}$$

The work also used the MRF (moving rotating frame) concept to simulate the propeller rotation effect. Still, due to the extension of its formulation, it was decided not to present it in the present text. However, a detailed explanation of MRF and all the equations in this section can be found in ANSYS [5].

4 Geometry

The geometry was developed in Solidworks, and for each blade, three sections were considered. All sections used the NACA2412 airfoil. The root section has a chord length of 1.8 cm, the midsection 2.8 cm, and the tip section 1.5 cm. The angles of the first two sections were chosen to optimize efficiency, as is done in conventional propellers. However, for the last section, a 90° angle was used to achieve the toroidal shape. Figure 2 shows the final geometry.

Figure 2. Propeller geometry

5 Operational Optimization

The first step is find a optimum operational point for the original propeller. This step is called operational optimization and the objective is to maximize the efficiency while using as the constraint that the power must remain within the range of 1200 to 1300 W. This power was based on OS Engine 55AX.

To achieve this objective, the optimization process will focus on two key design variables: rotation speed and advance ratio. The rotation speed must be maintained within the 5,000 to 10,000 rpm. Simultaneously, the advance ratio should be constrained between 1 and 3.

Three different optimization methodologies were employed to maximize the system's efficiency (η) under the given constraints: Multi-Objective Genetic Algorithm (MOGA) [6], Adaptive Multiple-Objective Optimization (AMO) [7], and Nonlinear Programming by Quadratic Lagrangian (NLPQL) [8]. Both MOGA and AMO began with 15 initial samples and generated 15 samples per iteration, configured with a Maximum Allowable Pareto Percentage of 99% and a Convergence Stability Percentage of 0.1%, and each allowed to run for a maximum of 10 iterations. NLPQL, on the other hand, used a Finite Difference Approximation method with a central difference approach, an allowable convergence threshold of 0.001, and a maximum of 20 iterations. For NLPQL, three separate runs were executed with initial conditions set at rotation speeds of 5000, 7000, and 10000 rpm, and advance ratios of 1, 2, and 3. This approach was important to ensure that the global maximum was achieved by thoroughly exploring the solution space.

For the simulations, the problem is divided into two domains: the stator and the rotor. The rotor, which contains the propeller, is a rotating domain, whereas the stator is a non-rotating domain. The stator domain includes a space where there is an interface with the rotor [9]. Both domains are cylindrical. The rotor has a diameter of 1.1 times the propeller's diameter and a height of 0.4 times the propeller's diameter, whereas the height and diameter of the stator domain are 8 times the propeller's diameter.

The meshes were generated in ANSYS Mesh. The element size of the rotor mesh was set to 0.1 m, a metric that automatically controls other mesh parameters. The capture curvature algorithm was used with a curvature angle of 5°, and the proximity algorithm was used with a proximity gap factor of 4 for edges and faces. The resulting mesh has 133,000 nodes and 741,161 elements, which is sufficient to ensure the achievement of good

results [9][10]. The average element quality was 0.83634, and the average skewness was 0.23036. All other parameters were automatically determined by the element size. Rotor mesh is shown in Figure 3.

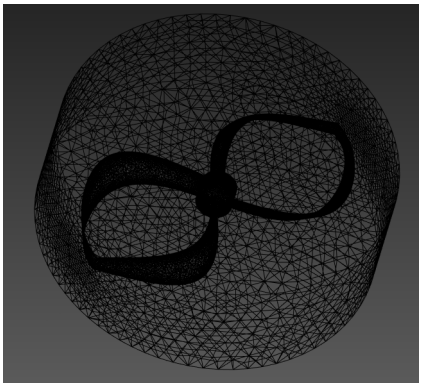

Figure 3. Mesh generated for rotor domain

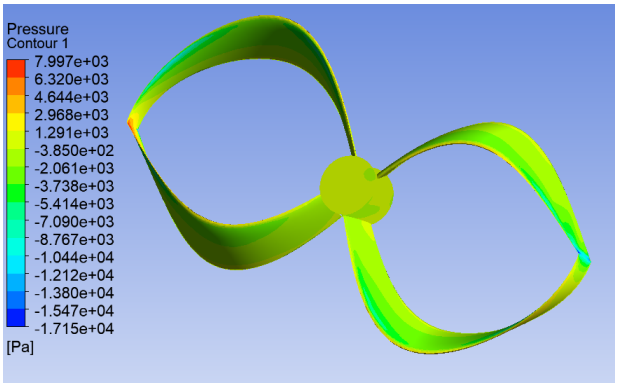

Figure 4. Relative pressure contours for propeller

The stator mesh was generated using an element size of 0.1 m and the mesh defeature algorithm. Due to the simplicity of this mesh, it was not necessary to use curvature and proximity algorithms. The resulting mesh had 7,530 nodes and 38,398 elements. The average element quality is 0.83658, and the skewness is 0.22949.

The simulations were conducted using CFX software and carried out in a steady-state regime. An inlet boundary was set on one of the faces of the stator to simulate the propeller's translation velocity. For the other stator's boundaries, open conditions with zero gauge pressure were applied. Interfaces between the domains were established. In the rotor domain, rotational speed was specified, and wall conditions were set on the faces of the propeller [9]. The relative pressure contour for the propeller is shown in Figure 4.The Mesh and CFX modules were coupled with the Direct Optimization module in the ANSYS Workbench environment, as shown in Figure 5.

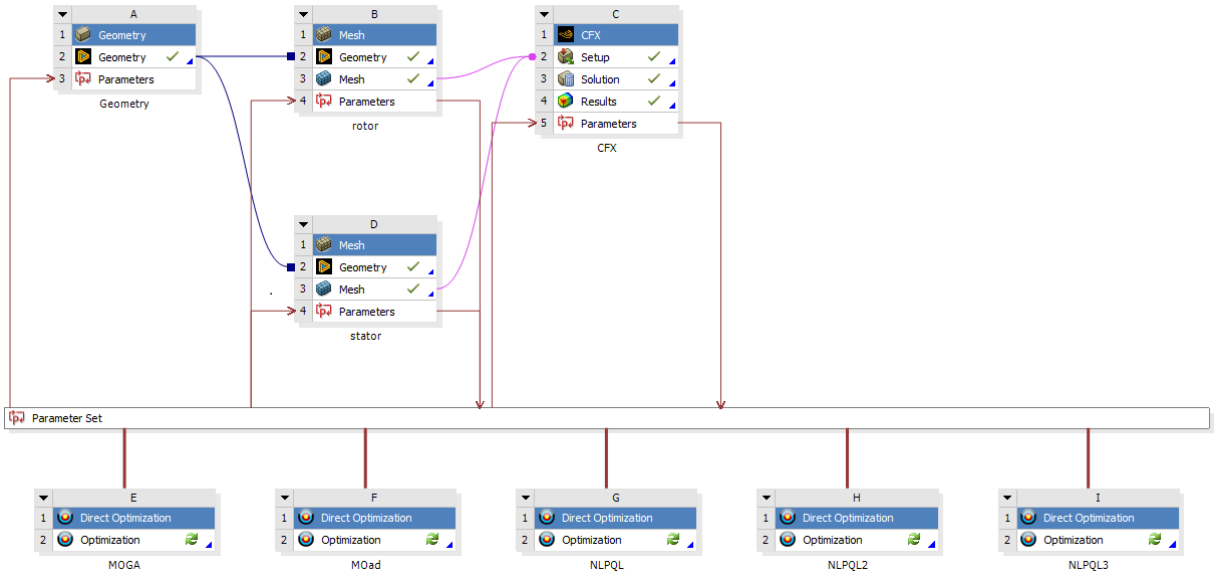

Figure 5. Workbench setup coupling optimization, mesh, and simulation

Table 1 shows the best candidates for each of the optimizations performed. Based on the presented data, it is concluded that the best candidate is number 5. For the simulations performed in this section, 4 cores of the 11th Gen Intel(R) Core(TM) i7-11800H @ 2.30GHz CPU were also used, with a total simulation time of approximately 3500 minutes.

6 Geometric optimization

For the geometric optimization, the geometry was parameterized using modular construction through Spaceclaim. Three scales, each in the x, y, and z axes, were used as parameters. Therefore, S_x acts in the radial direction

Table 1. Results obtained for operational optimization

Candidate	Optimizer	Rotation (rpm)	Advance ratio	Efficiency	Power (W)
1	MOGA	7994.6	1.7754	0.54289	1220.0
2	AMO	7994.6	1.7754	0.54289	1220.0
3	NLPQL	8148.4	1.7968	0.54314	1287.3
4	NLPQL	8005.8	1.7729	0.54287	1225.5
5	NLPQL	8084.8	1.8409	0.54321	1299.8

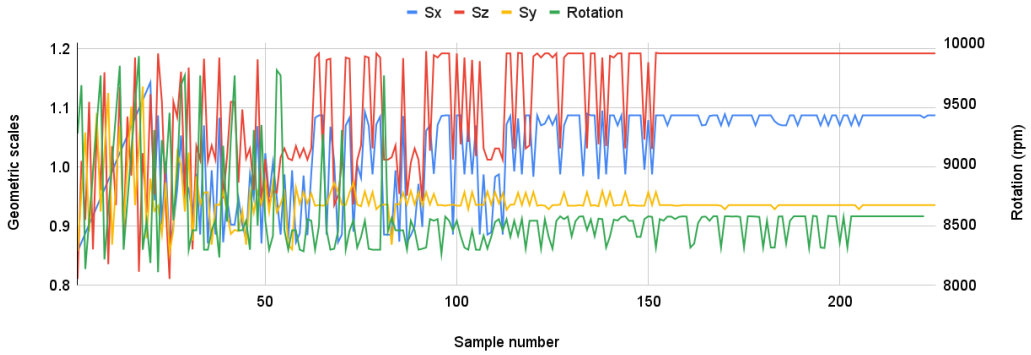

Figure 6. Design variables per sample number - MOGA

of the blade stretching, S_y in the radial direction perpendicular to the blade stretching, and S_z in the longitudinal height direction.

For the geometric optimization, the same mesh generation philosophies were used. However, since the dimensions of the propeller and, consequently, the dimensions of the domains change according to the geometric parameters, parameterizations were also used for the element size. These parameterizations are:

$$ElementSize = 0.1\sqrt[3]{S_x S_y S_z} \tag{11}$$

Through the parameterization of the element size, it is ensured that the number of elements and nodes in the meshes remain consistent, preventing larger propellers from having too many elements and smaller propellers from having too few. The dimensions of the domains were parameterized using the diameter, according to the relationships specified in the previous section.

The objective of the geometric optimization remains to maximize efficiency, while the power constraint remains the same. The rotational speed continues to be one of the optimization parameters, with limits between 8,000 and 10,000 rpm. The advance ratio is fixed at 1.8409, a value found to be optimal in the operational optimization. The other design variables are geometric: S_x and S_y, in the range of 0.85-1.15, and S_z, in the range of 0.8-1.2. In this group of simulations, the rotation grid interval was 1 and the geometric variables interval was 0.01.

Since the results for MOGA and AMO were similar, it was decided to use only MOGA at this stage, with a number of initial samples of 20, number of samples per iteration of 20, maximum allowable Pareto percentage of 99%, convergence stability percentage of 1%, and maximum number of iterations of 15. As NLPQL does not support the use of grid intervals, it was not used here. Instead, MISQP was used (Mixed Integer Sequential Quadratic Programming) [11]. MISQP was set with finite difference approximation central, allowable convergence of 0.1%, and a maximum number of iterations of 20.

As mentioned earlier, the meshes were parameterized and, therefore, their number of elements is variable. For the MOGA meshes, the rotating domain had an average of 693,281 elements with a standard deviation of 21,723 elements, while the stationary domain had an average of 39,434 elements with a standard deviation of 941 elements. For the MISQP, the rotating domain had an average of 740,470 elements with a standard deviation of 11,944 elements, while the stationary domain had an average of 37,408 elements with a standard deviation of 678 elements.

The best candidates for each of the geometric optimizations are shown in Table 2:

As shown, the best candidate was obtained by the MOGA optimizer. When comparing this candidate ($\eta = 0.58263$) with candidate 5 from the first stage ($\eta = 0.54321$), an increase in efficiency of more than 7% is observed. The increase in S_z was 19.2%, while S_x increased by 8.7% and S_y decreased by 6.5%, making the aspect ratio of

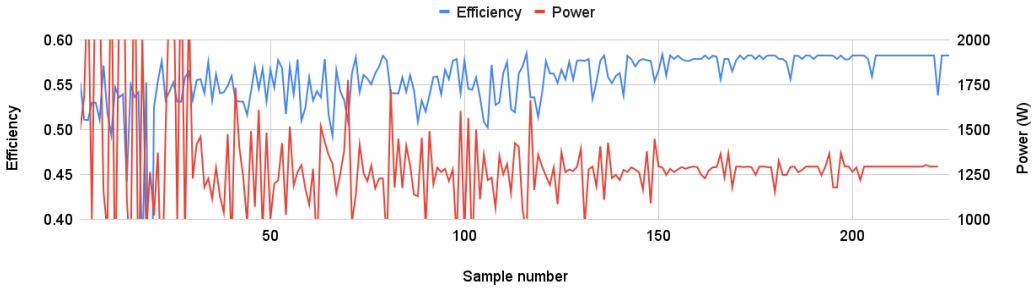

Figure 7. Efficiency and power constraint - MOGA

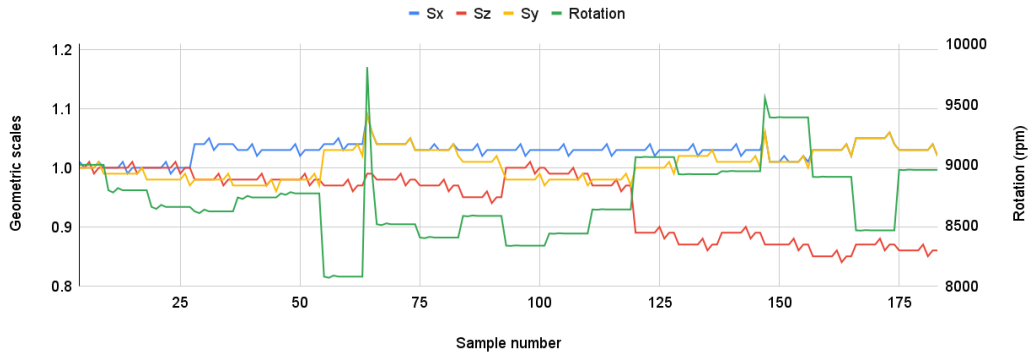

Figure 8. Design variables per sample number - MISQP

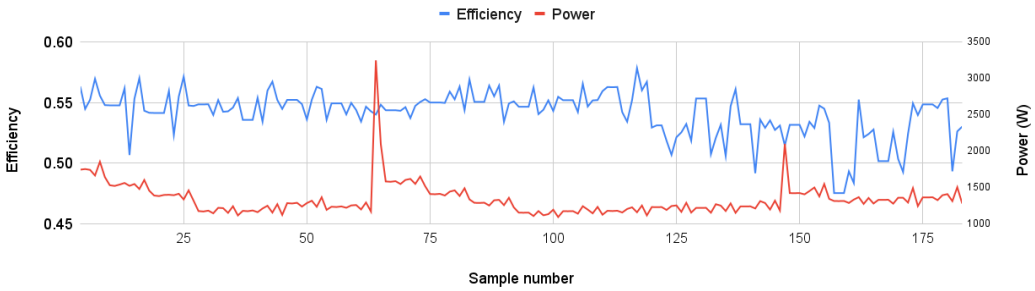

Figure 9. Efficiency and power constraint - MISQP

Table 2. Results obtained for geometric optimization

Candidate	Optimizer	S_x	S_y	S_z	Rotation (rpm)	Efficiency	Power (W)
1	MOGA	1.087	0.935	1.192	8556	0.58263	1294.0
2	MISP	1.031	1.020	0.869	8922	0.55329	1219.1

the propeller less elongated than the original. This behavior also indirectly increases the incidence angles of the propeller blades, as well as increases the size of the chord lengths. Through Figure 10, it is possible to compare the original propeller to the optimized one. For the simulations performed in this section, 4 cores of the 11th Gen Intel(R) Core(TM) i7-11800H @ 2.30GHz CPU were also used, with a total simulation time of approximately 7200 minutes.

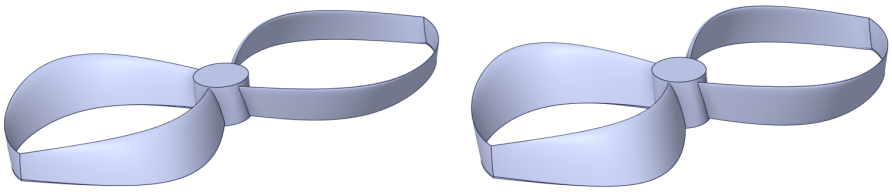

Figure 10. Original propeller on the left and optimized propeller on the right.

7 Conclusions

The present study proposed an optimization aimed at maximizing the efficiency of a toroidal propeller. An efficiency increase of just over 7% was achieved. Therefore, it is considered that the study met its objective. However, there are limitations. Initially, it can be mentioned that CFD analysis is quite reliable but has small discrepancies when compared to experimental tests [9]. For the presented work, the major limitation lies in the geometry rather than the CFD analysis. Ideally, the propeller should have all its characteristics parameterized, including chord and angles at all sections, as well as diameter and number of blades. This would allow for a much more comprehensive optimization, but the computational cost would be much higher.

Acknowledgements. This study was financed in part by the Coordenação de Aperfeiçoamento de Pessoal de Nível Superior - Brazil (CAPES) - Finance Code 001, CNPq (308105/2021-4, and 303221/2022-4), CAPES (Finance code 001), FAPEMIG (APQ-00869-22 and TEC PPM-00174-18)

Authorship statement. The authors hereby confirm that they are the sole liable persons responsible for the authorship of this work, and that all material that has been herein included as part of the present paper is either the property (and authorship) of the authors, or has the permission of the owners to be included here.

References

[1] MIT. Toroidal propeller, lincoln laboratory, 2022.
[2] X.-d. Vu, A.-t. Nguyen, T.-l. Nha, Q. Chu, and C.-t. Dınh. Numerical aerodynamic and aeroacoustic analysis of toroidal propeller designs. *International Journal of Aviation Science and Technology*, 2024.
[3] I. Gabriel and I. Simion. Performance of 3d printed conventional and toroidal propeller for small multirotor drones. *Journal of Industrial Design and Engineering Graphics*, vol. 18, n. 1, pp. 27–32, 2023.
[4] J. Brandt and M. Selig. Propeller performance data at low reynolds numbers. In *49th AIAA Aerospace Sciences Meeting including the New Horizons Forum and Aerospace Exposition*, pp. 1255, 2011.
[5] ANSYS. Ansys cfx-solver theory guide. *Ansys CFX Release*, 2024.
[6] T. Murata, H. Ishibuchi, and others. Moga: multi-objective genetic algorithms. In *IEEE international conference on evolutionary computation*, volume 1, pp. 289–294. IEEE Piscataway, 1995.
[7] S. Tickoo. Ansys workbench 2021 r1: A tutorial approach, 2021.
[8] K. Schittkowski. Nlpql: A fortran subroutine solving constrained nonlinear programming problems. *Annals of operations research*, vol. 5, pp. 485–500, 1986.
[9] E. V. Loureiro, N. L. Oliveira, P. H. Hallak, de F. Souza Bastos, L. M. Rocha, R. G. P. Delmonte, and de A. C. Castro Lemonge. Evaluation of low fidelity and cfd methods for the aerodynamic performance of a small propeller. *Aerospace Science and Technology*, vol. 108, pp. 106402, 2021.
[10] N. L. Oliveira, L. M. Rocha, P. H. Hallak, and M. A. Rendón. Influence of crosswinds on propellers perfomance, 2019.
[11] O. Exler, T. Lehmann, and K. Schittkowski. Misqp: A fortran subroutine of a trust region sqp algorithm for mixed-integer nonlinear programming-user's guide. *Report, Department of Computer Science*, 2012.